Journal of Statistical Physics, Vol. 73, Nos. 1/2, 1993

Collective Diffusion in a Lattice Gas Automaton

René H. van Roij[1,2] and Matthieu H. Ernst[1]

Received February 16, 1993; final May 13, 1993

We report on non-mean-field and ring-kinetic-theory calculations of both the momentum autocorrelation function and the collective diffusion coefficient in a diffusive lattice gas automaton. For both quantities the ring approximation is calculated exactly. A saddle point method yields a leading t^{-2} and a subleading $t^{-5/2}$ long-time tail in the momentum autocorrelation function. The ring kinetic corrections to the mean field value of the diffusion coefficient are in good agreement with computer simulations.

KEY WORDS: Collective diffusion; momentum autocorrelation; ring kinetic theory; long-time tails.

1. INTRODUCTION

Collective diffusion refers to the random motion of the center of mass $X(t)$ of all particles in systems where the total momentum $P_x(t)$ is not conserved, whereas self-diffusion or tagged particle diffusion is related to the random motion of a single particle.

For sufficiently long times such motion can be characterized by Einstein's formula for the mean-square displacement. In the former case one has $\langle (X(t)-X(0))^2 \rangle \simeq 2\Delta t$, where Δ is essentially the collective diffusion coefficient. In the latter case one has $\langle (x_s(t)-x_s(0))^2 \rangle \simeq 2D_s t$, where D_s is the coefficient of self-diffusion and x_s the spatial coordinate of the tagged particle.

The collective diffusion equation describes the time evolution of the probability distribution for X-displacements or the relaxation of spatial

[1] Institute for Theoretical Physics, University of Utrecht, 3508 TA Utrecht, The Netherlands.
[2] Present address: FOM Institute for Atomic and Molecular Physics, 1009 DB Amsterdam, The Netherlands.

822/73/1-2-4

inhomogeneities in the density distribution ρ on large spatial and temporal scales. It is the analog of the Navier–Stokes equation that describes the decay of the local momentum density $\rho \mathbf{u}$ in systems with momentum-conserving dynamics on similar scales.

Colloidal particles are one of the most important examples of interacting systems showing collective diffusion.[1] The lattice gas to be studied in this paper may be considered as a caricature of such a system. It has been introduced by Boghosian and Levermore[2] and represents a system of interacting particles whose dynamics contains the standard ingredients of lattice gas automata (LGA)—a collision step and a propagation step—and leads to diffusive behavior at the macroscopic level.

The goal of this paper is to investigate the consequences of the breakdown of the molecular chaos assumption, to analyze in a quantitative manner the importance of dynamic correlations on transport coefficients and time correlation functions in such systems, and to support the theoretical results by computer simulations. Recently the collective diffusion coefficient has also been studied by Taylor and Boghosian.[3]

The molecular chaos assumption leads to the standard Boltzmann or mean field equation. In a recent publication Kirkpatrick and Ernst[4] have developed the ring kinetic theory for LGA which enables us to calculate the ring diagrams or one-loop corrections to the Boltzmann value for the transport coefficients. The absence of molecular chaos is also responsible for long-time tails in the time correlation functions of the Green–Kubo formulas. Our exact evaluation of the ring diagrams at finite times allows us also to calculate the long-time tails in the momentum autocorrelation function $\langle P_x(t)\, P_x(0)\rangle$.

As is well known, the long-time tail in fluid-type models has the form $+at^{-d/2}$, where d is the dimensionality and a a positive constant. However, in purely diffusive systems, such as Lorentz gases with static scatterers or the present type of model for collective diffusion, the long-time tail has the form $-at^{-(d+2)/2}$. This difference is essentially caused by the absence, in purely diffusive systems, of a slow mode with a vector character, such as the shear modes in fluids.

The plan of this paper is as follows: in Section 2 the microdynamic equation is constructed, and a Green–Kubo formula derived for the coefficient of collective diffusion. Section 3 develops the mean field and the ring kinetic theory. The ring integral is evaluated analytically in Section 4 for all times. In Section 5 the asymptotic behavior is evaluated with the help of a saddle point method. Section 6 presents the comparison of theory and computer simulations, and we conclude in Section 7 with a brief discussion.

2. DIFFUSIVE LGA

Consider a two-dimensional square lattice $\mathscr{L}$ consisting of $V = L \times L$ sites with periodic boundary conditions. Every node $\mathbf{r} \in \mathscr{L}$ has four nearest neighbors $\mathbf{r} + \mathbf{c}_i$ $(i = 0,..., 3)$. The velocity channels $\mathbf{c}_i$ are $\mathbf{c}_0 = (1, 0)$, $\mathbf{c}_1 = (0, 1)$, $\mathbf{c}_2 = (-1, 0)$, and $\mathbf{c}_3 = (0, -1)$. The direction parallel to $\mathbf{c}_0$ will be referred to as the x direction.

The lattice contains ρV particles. The microstate of the system at time t $(t = 0, 1, 2,...)$ is described by the set of (precollision) occupation numbers $\{n_i(\mathbf{r}, t)\}$, where $n_i(\mathbf{r}, t) = 1$ or 0 denotes the presence or absence of a moving particle at site $\mathbf{r}$ with velocity $\mathbf{c}_i$ at time t just before collision. Thus there are $2^4 = 16$ possible states per node.

The time evolution of the LGA is deterministic. It consists of collisions and propagation. The collisions change the precollision occupation numbers $n_i(\mathbf{r}, t)$ instantaneously into postcollision occupation numbers $n_i'(\mathbf{r}, t)$, where collision rules are illustrated in Fig. 1. If two particles meet with input velocities at right angles, their velocities are reversed, provided the output channels are empty. In all other cases the velocities of the particles remain unchanged. After the collision step follows the propagation step, in which a particle in channel $\mathbf{c}_i$ at node $\mathbf{r}$ is moved to position $\mathbf{r} + \mathbf{c}_i$, so that $n_i(\mathbf{r} + \mathbf{c}_i, t + 1) = n_i'(\mathbf{r}, t)$.

Formally the time evolution is described by the microdynamic equation

$$n_i(\mathbf{r} + \mathbf{c}_i, t + 1) = n_i(\mathbf{r}, t) + I_i(n(\mathbf{r}, t)) \qquad (i = 0,..., 3) \qquad (2.1)$$

where a single time step in the evolution of the automaton consists of the combined collision and propagation step. In the present paper we only use the precollision occupation numbers $n_i(\mathbf{r}, t)$, and discard the postcollision ones, $n_i'(\mathbf{r}, t)$. Of course a completely equivalent description of the dynamics might be given in postcollision occupation numbers.

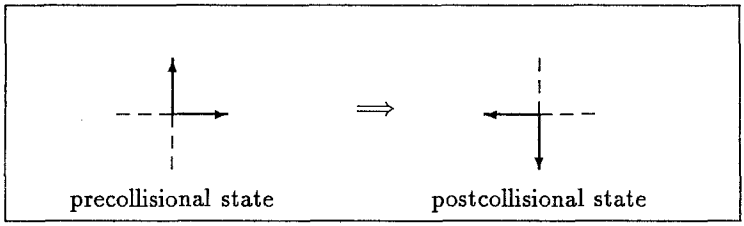

Fig. 1. Basic collision rules. Arrows represent occupied channels, dashed lines empty ones.

The nonlinear collision operator can be constructed from Fig. 1 and reads

$$\begin{aligned} I_i(n) &= n_{i+2}n_{i+1}\bar{n}_i\bar{n}_{i+3} - n_i n_{i+3}\bar{n}_{i+2}\bar{n}_{i+1} \\ &\quad + n_{i+2}n_{i+3}\bar{n}_i\bar{n}_{i+1} - n_i n_{i+1}\bar{n}_{i+2}\bar{n}_{i+3} \\ &= (n_{i+2} - n_i)(n_{i+1} + n_{i+3} - 2n_{i+1}n_{i+3}) \end{aligned} \tag{2.2}$$

where $\bar{n}_i = (1 - n_i)$.

One of the consequences of this purely local collision rule is that the total number of particles moving along any line (either horizontal or vertical) is conserved, whereas total momentum is not conserved in general. There are many sites with noninteracting two-, three-, and four-particle encounters that trivially conserve the total momentum *per node*. It is the frequency of the interacting collisions in Fig. 1 that determines the mean free time t_o and the mean free path l_o. The total momentum is a decaying quantity on spatial and temporal scales large compared to l_o and t_o, respectively.[3]

The lack of conservation of momentum and the existence of so many spurious invariants disqualify this cellular automaton as a fluid model. The density of particles moving along a line satisfies in fact a one-dimensional *diffusion equation*, as was shown in ref. 2 in a mean field picture.

The equilibrium density is the stationary solution of Eq. (2.1), i.e., $I_i(n(\mathbf{r}, \infty)) = 0$. This yields $n_i(\mathbf{r}, \infty) = f_x(\mathbf{r})$ $(i = 0, 2)$ or $f_y(\mathbf{r})$ $(i = 1, 3)$ in view of the square symmetry. In the present case the initial conditions are chosen such that the number of y particles (i.e., particles moving in the $+y$ or $-y$ direction) on a line parallel to the y axis is independent of x and vice versa. The equilibrium average $\langle n_i(\mathbf{r}, t)\rangle$ is therefore independent of position and time. The reduced densities are defined as

$$\langle n_i(\mathbf{r}, t)\rangle = f_i = \begin{cases} f_x & \text{if } i = 0, 2 \\ f_y & \text{if } i = 1, 3 \end{cases} \tag{2.3}$$

where f_x and f_y are determined by the initial conditions. The total particle density ρ is given by $\rho = 2(f_x + f_y)$.

In the sequel we need an expansion of the collision operator $I_i(n)$ in fluctuations around equilibrium. We define

$$\delta n_i(\mathbf{r}, t) \equiv n_i(\mathbf{r}, t) - \langle n_i(\mathbf{r}, t)\rangle \tag{2.4}$$

[3] In terms of the dimensionless units used here we have according to Eq. (2.6) that $t_0 = D_x$ varies between 0.5 ($\rho = 0.5$) and 6 ($\rho = 0.05$), and corresponding values for l_o.

Combining Eqs. (2.4) and (2.3) with (2.2) gives

$$I_i(n) = \Omega_{ij}\delta n_j + \sum_{\lambda=2}^{3} \Omega^{(\lambda)}_{ii_1\cdots i_\lambda}\delta n_{i_1}\cdots\delta n_{i_\lambda} \tag{2.5}$$

where the Einstein summation convention is used for repeated indices. The term $\Omega^{(1)}_{ij} = \Omega_{ij}$ is the linearized Boltzmann collision operator. It satisfies $\Omega_{ij} = \Omega_{ji}$. Furthermore, $\Omega^{(\lambda)}_{ii_1\cdots i_\lambda}$ is symmetric in the labels $i_1\cdots i_\lambda$ for $\lambda = 2, 3$ and vanishes if at least two indices out of $(i_1\cdots i_\lambda)$ are equal. The terms with $\lambda = 0, 4$ [the zeroth- and fourth-order terms in Eq. (2.5)] vanish.

The average number density $\bar{\rho}_x(\mathbf{r}, t)$ of x particles satisfies a diffusion equation, $\partial_t\bar{\rho}_x = D_x\nabla_x^2\bar{\rho}_x$, because the number of x particles is conserved, but not its flux. If we apply linear response theory to this system according to refs. 5 and 6, the *collective* diffusion coefficient D_x is obtained in the form of a Green–Kubo formula

$$D_x = \sum_{t=0}^{\infty}{}^{*}\, \phi_x(t) \tag{2.6}$$

where the asterisk indicates that the term with $t = 0$ has a weight 1/2. The momentum autocorrelation function $\phi_x(t)$ is defined as

$$\phi_x(t) = \frac{\langle P_x(t)\, P_x(0)\rangle}{\langle (\delta N_x)^2\rangle} \tag{2.7}$$

Here $P_x(t)$ is the total x momentum at time t and N_x the total number of x particles, with fluctuation $\delta N_x = N_x - \langle N_x\rangle$:

$$\begin{aligned} P_x(t) &= \sum_{\mathbf{r}i} c_{xi} n_i(\mathbf{r}, t) \\ N_x(t) &= \sum_{\mathbf{r}i} \rho_{xi} n_i(\mathbf{r}, t) \end{aligned} \tag{2.8}$$

with $c_{xi} = \delta_{i0} - \delta_{i2}$ and $\rho_{xi} = \delta_{i0} + \delta_{i2}$. The Green–Kubo formula, Eqs. (2.6) and (2.7), for the collective diffusion coefficient can be rewritten as an Einstein relation,

$$\langle (X(t) - X(0))^2\rangle = 2\langle (\delta N_x)^2\rangle\, D_x t \qquad (t \to \infty) \tag{2.9}$$

where $X(t)$ is the x component of the center of mass. The collective diffusion coefficient D_x describes the growth of the mean-square displacement of the center of mass of all particles moving in the x direction. The collective diffusion coefficients D_x and D_y should be distinguished from the self-

diffusion coefficient $D_x^s = \sum_t^* \langle v_x(t)\, v_x(0)\rangle$, where $v_x(t)$ is the x velocity of a single tagged particle.[7]

Next we express the momentum autocorrelation function in terms of the kinetic propagator Γ. It follows from Eq. (2.8) that

$$\langle P_x(t)\, P_x(0)\rangle = V \sum_{\mathbf{r}} \sum_{ij} c_{xi} \langle \delta n_i(\mathbf{r}, t)\, \delta n_j(\mathbf{0}, 0)\rangle\, c_{xj} \tag{2.10}$$

where we have used translational invariance of ensemble averages. Exploiting the fact that initially no spatial correlations are present, we see that the equal-time correlation is given by

$$\langle \delta n_i(\mathbf{r}, 0)\, \delta n_j(\mathbf{0}, 0)\rangle = \delta(\mathbf{r}, 0)\, \delta_{ij} \langle (\delta n_i)^2\rangle \tag{2.11}$$

Here $\delta(\mathbf{r}, \mathbf{r}')$ is the two-dimensional Kronecker delta. The Fermi character of the particles gives

$$\langle (\delta n_i)^2\rangle = f_i(1 - f_i) \equiv \kappa_i \tag{2.12}$$

so that the normalization of Eq. (2.7) is $\langle (\delta N_x)^2\rangle = 2V_{\kappa_x}$, with $\kappa_x \equiv \kappa_0 = \kappa_2$. Combining this with Eqs. (2.10) and (2.7) yields

$$\phi_x(t) = \tfrac{1}{2} \sum_{\mathbf{r}} \sum_{ij} c_{xi} \tilde{\Gamma}_{ij}(\mathbf{r}, t)\, c_{xj} \tag{2.13}$$

where the kinetic propagator is defined as

$$\tilde{\Gamma}_{ij}(\mathbf{r}, t) = \frac{1}{\kappa_j} \langle \delta n_i(\mathbf{r}, t)\, \delta n_j(\mathbf{0}, 0)\rangle \tag{2.14}$$

Note that *no* summation is understood here and that the normalization is chosen such that $\tilde{\Gamma}_{ij}(\mathbf{r}, 0) = \delta_{ij}\delta(\mathbf{r}, \mathbf{0})$.

In order to proceed, it is convenient to use Fourier transforms:

$$n_i(\mathbf{q}, t) \equiv \sum_{\mathbf{r}} \exp[-i\mathbf{q}\cdot\mathbf{r}]\, \delta n_i(\mathbf{r}, t) \tag{2.15}$$

so that

$$\begin{aligned} \Gamma_{ij}(\mathbf{q}, t) &\equiv \sum_{\mathbf{r}} \exp[-i\mathbf{q}\cdot\mathbf{r}]\, \tilde{\Gamma}_{ij}(\mathbf{r}, t) \\ &= \frac{1}{V\kappa_j} \langle n_i(\mathbf{q}, t)\, n_j^*(\mathbf{q}, 0)\rangle \end{aligned} \tag{2.16}$$

where the asterisk denotes complex conjugation. Equation (2.16) allows us to write Eq. (2.13) as

$$\phi_x(t) = \tfrac{1}{2} \sum_{ij} c_{xi} \Gamma_{ij}(\mathbf{q} = \mathbf{0}, t)\, c_{xj} \tag{2.17}$$

The calculation of $\phi_x(t)$ and D_x has been reduced to the calculation of the propagator $\Gamma(\mathbf{q}, t)$. First we will determine Γ in Boltzmann approximation, thereafter we will apply ring kinetic theory to calculate corrections.

3. MEAN FIELD THEORY AND BEYOND

In this section we briefly discuss the results from mean field theory and outline the calculations of the one-loop corrections to the kinetic propagator. Technically the mean field or Boltzmann approximation consists of neglecting all quadratic and higher-order terms in δn in Eq. (2.5).[4] This can be interpreted as a mean field approximation, because a fluctuation δn from equilibrium only interacts with the average field of all other particles while no interaction with other fluctuations are taken into account. If we apply the Boltzmann approximation to the equation of motion (2.1), we obtain

$$\delta n_i(\mathbf{r}, t+1) = S_i^{-1}(\delta_{ij} + \Omega_{ij})\, \delta n_j(\mathbf{r}, t) \tag{3.1}$$

where $S_i n_j(\mathbf{r}) = n_j(\mathbf{r} + \mathbf{c}_i)$ is the free streaming operator. We proceed by Fourier transforming Eq. (3.1) and iterating it t times. This yields the solution

$$n_i(\mathbf{q}, t) = [S^{-1}(\mathbf{q})(\mathbf{1} + \Omega)]^t_{ij}\, n_j(\mathbf{q}, 0) \tag{3.2}$$

where $S_{ij}(\mathbf{q}) = S_i(\mathbf{q})\, \delta_{ij} = \delta_{ij} \exp[i\mathbf{q} \cdot \mathbf{c}_i]$ is considered as a diagonal matrix. The Boltzmann approximation for $\Gamma(\mathbf{q}, t)$ becomes then

$$\Gamma^0_{ij}(\mathbf{q}, t) = [S^{-1}(\mathbf{q})(\mathbf{1} + \Omega)]^t_{ij} \tag{3.3}$$

and for the momentum autocorrelation function

$$\phi^0_x(t) = \tfrac{1}{2} c_x \cdot (\mathbf{1} + \Omega)^t \cdot c_x \tag{3.4}$$

where an obvious vector and matrix notation has been used. From the explicit form (A.1) for the 4×4 matrix Ω_{ij} in Appendix A one verifies that the four-vector c_{xi} is an eigenvector: $\Omega c_x = -4\kappa_y c_x$. Therefore Eq. (3.4) can be reduced to

$$\phi^0_x(t) = (1 - \omega_x)^t \qquad (\omega_x = 4\kappa_y) \tag{3.5}$$

because $c_x \cdot c_x = 2$. Note that $0 \leqslant \omega_x \leqslant 1$, so that $\phi_x^0(t)$ is nonnegative for all t. Combining Eqs. (3.4) and (2.6) gives the Boltzmann approximation for D_x:

$$D_x^0 = \sum_{t=0}^{\infty} (1-\omega_x)^t - \frac{1}{2} = \frac{1}{\omega_x} - \frac{1}{2} \tag{3.6}$$

which is always positive. Figure 2 shows the Boltzmann result as a solid line.

Next we calculate $\Gamma_{ij}(\mathbf{q}, t)$ beyond the Boltzmann approximation by taking into account the higher-order terms in the expansion of $I_i(n)$ in Eq. (2.5). This requires the calculation of the one-loop corrections, i.e., ring collision diagrams, in the kinetic propagator $\Gamma_{ij}(\mathbf{q}, t)$. A similar program has been carried out in ref. 4 for the standard cellular automata fluids with momentum conservation. As all formal manipulations for the diffusive and the fluid type lattice gas automata are identical, we only quote the result:

$$\Gamma_{ij}(\mathbf{q}, t) = \Gamma_{ij}^0(\mathbf{q}, t) + \Gamma_{ij}^{(2)}(\mathbf{q}, t) + \Gamma_{ij}^{(3)}(\mathbf{q}, t)$$

$$= \quad ——— \quad + \quad —◯— \quad + \quad —⊖— \tag{3.7}$$

A single line represents the Boltzmann propagator Γ^0 defined in Eq. (3.3). The next terms consist of two external Γ^0-propagators and a ring diagram with λ parallel lines ($\lambda = 2, 3$) representing internal Γ^0-propagators:

$$\Gamma_{ij}^{(\lambda)} \kappa_j = \Gamma_{ik}^0(\mathbf{q}, t)\, S_k^{-1}(\mathbf{q}) \otimes \mathscr{R}_{kl}^{(\lambda)}(\mathbf{q}, t) \otimes \Gamma_{lj}^0(\mathbf{q}, t) \tag{3.8}$$

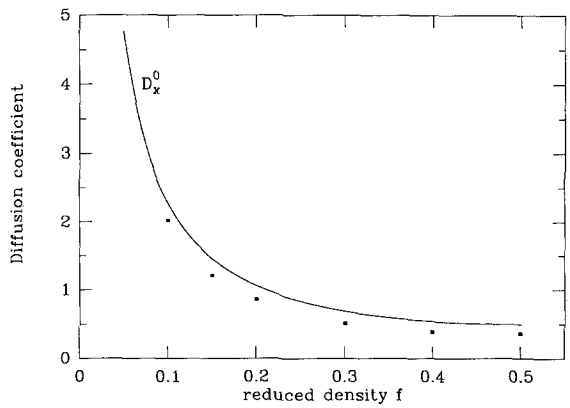

Fig. 2. Collective diffusion coefficient D_x versus reduced density $f = f_x = f_y$. The mean field value (solid line) is compared with computer simulations (squares) measured in a system of 200×200 sites.

where no summation over j is implied. The ring diagrams are

$$\mathscr{R}_{ij}^{(\lambda)}(\mathbf{q}, t) = \frac{\lambda!}{V^{\lambda-1}} \sum_{\mathbf{q}_1 \cdots \mathbf{q}_\lambda} \delta(\mathbf{q}, \mathbf{q}_1 + \mathbf{q}_2 + \cdots + \mathbf{q}_\lambda) \times \Omega_{ii_1 \cdots i_\lambda}^{(\lambda)} \Omega_{jj_1 \cdots j_\lambda}^{(\lambda)} \prod_{p=1}^{\lambda} (\Gamma_{i_p j_p}^{0}(\mathbf{q}_p, t)\, S_{j_p}^{-1}(\mathbf{q}_p)\, \kappa_{j_p}) \tag{3.9}$$

Here $\otimes$ denotes a time convolution, defined as

$$A(t) \otimes B(t) = \sum_{\tau=0}^{t-1} A(\tau)\, B(t-\tau-1) \tag{3.10}$$

and $\Omega_{ii_1 \cdots i_\lambda}^{(\lambda)}$ with $\lambda = 2, 3$ represents the vertex functions with one ingoing line (labeled i) and λ outgoing lines (labeled $i_1 \cdots i_\lambda$), as defined in Eq. (2.5) and calculated in Appendix A. We also point out that the double convolution in Eq. (3.8) vanishes for $t \leqslant 2$, because each factor in the convolution requires at least one time step since $\mathscr{R}_{ij}^{(\lambda)}(\mathbf{q}, 0)$ vanishes. From this observation we conclude immediately that the Boltzmann approximation for $\Gamma(\mathbf{q}, t)$, and consequently also for $\phi_x(t)$, is exact for $0 \leqslant t \leqslant 2$.

The ring approximation for the momentum autocorrelation function $\phi_x(t)$ in Eq. (2.17),

$$\phi_x(t) = \phi_x^0(t) + \phi_x^{(2)}(t) + \phi_x^{(3)}(t) \tag{3.11}$$

only involves the $(\mathbf{q} = \mathbf{0})$ component of the propagator $\Gamma_{ij}(\mathbf{q}, t)$. The first term in Eq. (3.11) yields the Boltzmann approximation $\phi_x^0(t)$ in Eq. (3.5). The ring terms can be written as

$$\begin{aligned} \phi_x^{(\lambda)}(t) &= \frac{1}{2} \sum_{ij} c_{xi} \Gamma_{ij}^{(\lambda)}(\mathbf{q} = \mathbf{0}, t)\, c_{xj} \\ &= \frac{1}{2\kappa_x} \sum_{\tau=1}^{t-2} \tau(1-\omega_x)^{\tau-1}\, c_{xi} \mathscr{R}_{ij}^{(\lambda)}(\mathbf{0}, t-\tau-1)\, c_{xj} \end{aligned} \tag{3.12}$$

where the relations

$$\begin{aligned} \Gamma^0(\mathbf{0}, t)\, \mathbf{c}_x &= (1-\omega_x)^t\, \mathbf{c}_x \\ \Gamma^0(\mathbf{0}, t) \otimes \Gamma^0(\mathbf{0}, t)\, \mathbf{c}_x &= t(1-\omega_x)^{t-1}\, \mathbf{c}_x \end{aligned} \tag{3.13}$$

have been used. Similarly, the ring corrections to the Boltzmann diffusion coefficient (3.6) follow from the Green–Kubo formula, (2.6) and (3.11), as

$$D_x = D_x^0 + D_x^{(2)} + D_x^{(3)} \tag{3.14}$$

with

$$D_x^{(\lambda)} = (2\kappa_x \omega_x^2)^{-1} \sum_{t=1}^{\infty} c_{xi} \mathscr{R}_{ij}^{(\lambda)}(\mathbf{0}, t)\, c_{xj} \qquad (\lambda = 2, 3) \tag{3.15}$$

4. EXACT CALCULATION OF THE RING INTEGRALS

In this section we present an exact calculation of the ring integrals,

$$R^{(\lambda)}(t) \equiv c_{xi} \mathscr{R}_{ij}^{(\lambda)}(\mathbf{0}, t)\, c_{xj} \tag{4.1}$$

and hence of $\phi_x^{(\lambda)}(t)$ from Eq. (3.12). First we will concentrate on $\lambda = 2$. The extension to $\lambda = 3$ is straightforward. From the representation of the function

$$\delta(\mathbf{r}, \mathbf{r}') = \frac{1}{V} \sum_{\mathbf{q}} \exp[i\mathbf{q} \cdot (\mathbf{r} - \mathbf{r}')] \tag{4.2}$$

the diagonal form of $S(\mathbf{q})$, and the definitions of $\Gamma^0(\mathbf{q}, t)$ in (3.3) and $\mathscr{R}_{ij}^{(\lambda)}(\mathbf{q}, t)$ in (3.9), one obtains

$$\begin{aligned} R^{(2)}(t) &= \frac{2}{V} A_{i_1 i_2}^{(2)} A_{j_1 j_2}^{(2)} \sum_{\mathbf{q}} \Gamma_{i_1 j_1}^0(\mathbf{q}, t)\, S_{j_1}^{-1}(\mathbf{q})\, \kappa_{j_1} \\ &\quad \times \Gamma_{i_2 j_2}^0(-\mathbf{q}, t)\, S_{j_2}^{-1}(-\mathbf{q})\, \kappa_{j_2} \\ &= 2A_{i_1 i_2}^{(2)} A_{j_1 j_2}^{(2)} \kappa_{j_1} \kappa_{j_2} \delta(\mathbf{r}_{i_1 j_1 \{k\}_t}, \mathbf{r}_{i_2 j_2 \{m\}_t}) \\ &\quad \times (\mathbf{1} + \Omega)_{i_1 k_1} (\mathbf{1} + \Omega)_{k_1 k_2} \cdots (\mathbf{1} + \Omega)_{k_{t-1} j_1} \\ &\quad \times (\mathbf{1} + \Omega)_{i_2 m_1} (\mathbf{1} + \Omega)_{m_1 m_2} \cdots (\mathbf{1} + \Omega)_{m_{t-1} j_2} \end{aligned} \tag{4.3}$$

where

$$\begin{aligned} A_{jk}^{(2)} &\equiv c_{xi} \Omega_{ijk}^{(2)} \\ \mathbf{r}_{ij\{k\}_t} &\equiv \mathbf{c}_i + \mathbf{c}_j + \mathbf{c}_{k_1} + \cdots + \mathbf{c}_{k_{t-1}} \end{aligned} \tag{4.4}$$

Because the matrix elements Ω_{ii+1}, Ω_{ii+3}, $A_{ii}^{(2)}$, and $A_{ii+2}^{(2)}$ vanish (see Appendix A), the vectors $\mathbf{r}_{i_1 j_1 \{k\}_t}$ and $\mathbf{r}_{i_2 j_2 \{m\}_t}$ in Eq. (4.3) are perpendicular to each other. As a consequence

$$\delta(\mathbf{r}_{i_1 j_1 \{k\}_t}, \mathbf{r}_{i_2 j_2 \{m\}_t}) = \delta(\mathbf{r}_{i_1 j_1 \{k\}_t}, \mathbf{0})\, \delta(\mathbf{r}_{i_2 j_2 \{m\}_t}, \mathbf{0})$$

in Eq. (4.3). It therefore factorizes into

$$R^{(2)}(t) = 2\kappa_x \kappa_y A_{i_1 i_2}^{(2)} Q_{i_1 j_1}(t)\, Q_{i_2 j_2}(t)\, A_{j_1 j_2}^{(2)} \tag{4.5}$$

with

$$Q_{ij}(t) \equiv (\mathbf{1}+\Omega)_{ik_1}(\mathbf{1}+\Omega)_{k_1k_2}\cdots(\mathbf{1}+\Omega)_{k_{t-1}j}\,\delta(\mathbf{0}, \mathbf{r}_{ij\{k\}_t}) \tag{4.6}$$

Recall that a summation over all intermediate k_n values satisfying the δ-function constraint is understood in Eq. (4.6). We already conclude that the ring integral $R^{(2)}(t)$ vanishes for *even* t, since $\mathbf{r}_{ij\{k\}_t}$ in Eq. (4.4) contains an *odd* number of $\mathbf{c}_i$ and is therefore nonvanishing.

In Appendix A we see that the only nonvanishing elements of $(\mathbf{1}+\Omega)$ are the virtual collision terms (ii) and the real collision terms $(ii+2)$, where $(\mathbf{1}+\Omega)_{ii} = 1-2\kappa_{i+1}$ and $(\mathbf{1}+\Omega)_{ii+2} = 2\kappa_{i+1}$. Therefore, if $(\mathbf{1}+\Omega)_{k_nk_{n+1}}$ corresponds to a real collision, then $\mathbf{c}_{k_n} = -\mathbf{c}_{k_{n+1}}$. If $(\mathbf{1}+\Omega)_{k_nk_{n+1}}$ is a virtual collision element, then $\mathbf{c}_{k_n} = \mathbf{c}_{k_{n+1}}$. This observation enables us to decompose Eq. (4.6) into terms with a fixed number, say σ, of real collisions and consequently $t-\sigma$ virtual collisions, where we sum over all possible values of σ. Suppose the t_1th, t_2th,..., t_σth terms in the product of $(\mathbf{1}+\Omega)$'s in Eq. (4.6) correspond to real collisions. Then, defining $t_0 = 0$ and $t_{\sigma+1} = t+1$, we observe that between t_{i-1} and t_i $(i = 1,..., \sigma+1)$ only virtual collisions occur, so that for t odd and $\tau_i = t_i - t_{i-1}$:

$$\begin{aligned}
Q_{ij}(t) = \delta_{ji+2} \sum_{\sigma=1}^{t}{}^{(-)} (1-2\kappa_{i+1})^{t-\sigma} \\
\times (2\kappa_{i+1})^{\sigma} \sum_{\tau_1=1}^{\infty} \cdots \sum_{\tau_{\sigma+1}=1}^{\infty} [\delta(T_\sigma, t+1) \\
\times \delta(\tau_1 - \tau_2 + \tau_3 - \cdots + \tau_\sigma - \tau_{\sigma+1}, 0)] \\
+ \delta_{ji} \sum_{\sigma=2}^{t-1}{}^{(+)} (1-2\kappa_{i+1})^{t-\sigma} \\
\times (2\kappa_{i+1})^{\sigma} \sum_{\tau_1=1}^{\infty} \cdots \sum_{\tau_{\sigma+1}=1}^{\infty} [\delta(T_\sigma, t+1) \\
\times \delta(\tau_1 - \tau_2 + \tau_3 - \cdots - \tau_\sigma + \tau_{\sigma+1}, 0)]
\end{aligned} \tag{4.7}$$

Here $T_\sigma = \tau_1 + \tau_2 + \cdots + \tau_{\sigma+1}$. We have distinguished between even $(+)$ and odd $(-)$ numbers of σ, because the closed polygon condition differs slightly for the two cases. Note that we have $j = i+2$ for odd σ, and $j = i$ for even σ. Using the relation $\delta(a, b)\,\delta(a+b, 2T) = \delta(a, T)\,\delta(b, t)$, we find that the $(\sigma+1)$-tuple sum over the τ's in Eq. (4.7) factorizes into two independent sums, with the result

$$Q_{ij}(t) = \mathrm{odd}(t)\left[\delta_{ji+2}\sum_{\sigma=1}^{t}{}^{(-)}(1-2\kappa_{i+1})^{t-\sigma}(2\kappa_{i+1})^{\sigma} f^2\left(\frac{\sigma+1}{2}, \frac{t+1}{2}\right)\right.$$
$$\left. + \delta_{ij}\sum_{\sigma=2}^{t-1}{}^{(+)}(1-2\kappa_{i+1})^{t-\sigma}(2\kappa_{i+1})^{\sigma} f\left(\frac{\sigma}{2}, \frac{t+1}{2}\right) f\left(\frac{\sigma+2}{2}, \frac{t+1}{2}\right)\right]$$
$$\equiv \mathrm{odd}(t)\left[\delta_{ji+2} K\left(2\kappa_{j+1}, \frac{t+1}{2}\right) + \delta_{ij} L\left(2\kappa_{j+1}, \frac{t+1}{2}\right)\right] \tag{4.8}$$

Here $\mathrm{odd}(t)$ vanishes for t even and equals unity for t odd and

$$f(k, n) \equiv \sum_{\tau_1=1}^{\infty} \cdots \sum_{\tau_k=1}^{\infty} \delta(n; \tau_1 + \tau_2 + \cdots + \tau_k) \quad k, n \text{ integer}$$
$$K(\lambda, t) \equiv (1-\lambda)^{2t-1} \sum_{s=1}^{t} \left(\frac{\lambda}{1-\lambda}\right)^{2s-1} f^2(s, t) \tag{4.9}$$
$$L(\lambda, t) \equiv (1-\lambda)^{2t-1} \sum_{s=1}^{t-1} \left(\frac{\lambda}{1-\lambda}\right)^{2s} f(s, t) f(s+1, t)$$

We observe that $0 \leqslant \lambda \leqslant 1/2$. Neither the sum variable s nor the time variable t is restricted to either odd or even integers.

We calculate the combinatorial factor $f(k, n)$, defined in expression (4.9), using the *generating function:*

$$G(k, z) \equiv \sum_{n=k}^{\infty} z^n f(k, n)$$
$$= \left[\frac{z}{1-z}\right]^k \tag{4.10}$$
$$= z^k \sum_{n=0}^{\infty} \frac{(k+n-1)!}{n!\,(k-1)!} z^n$$

Here Newton's binomial formula has been used. Introducing the Γ-function, with $\Gamma(n) = (n-1)!$ for integer n, we see from Eq. (4.10) that

$$f(k, n) = \frac{\Gamma(n)}{\Gamma(k)\,\Gamma(n-k+1)} \tag{4.11}$$

Note that $f(k, n)$ vanishes for $n < k$. Since $f(k, n)$ is known explicitly, the expressions (4.9) for the functions $K(\lambda, t)$ and $L(\lambda, t)$ are explicitly known as well. From the structure of matrix $A^{(2)}$ (Appendix A) and expression (4.5) of the ring integral, we see that

$$R^{(2)}(t) = -16\kappa_x\kappa_y(1-2f_y)^2\,\mathrm{odd}(t)\,F\left(\frac{t+1}{2}\right) \tag{4.12}$$

where

$$F(t) = [K(2\kappa_x, t) + L(2\kappa_x, t)][K(2\kappa_y, t) - L(2\kappa_y, t)] \tag{4.13}$$

We have calculated the ring integral $R^{(2)}(t)$ in terms of a function F, which is explicitly known in terms of finite sums [see Eqs. (4.13) and (4.9)]. Inserting the result into expression (3.12) for $\phi_x^{(2)}(t)$ yields

$$\phi_x^{(2)}(t) = -8(1-2f_y)^2 \kappa_y \sum_{\tau=1}^{t-2} \tau(1-\omega_x)^{\tau-1} \operatorname{odd}(t-\tau-1) F\left(\frac{t-\tau}{2}\right) \tag{4.14}$$

The function $\phi_x^{(3)}(t)$ can be calculated in analogous manner. Again our starting point is Eq. (3.12), but now we take $\lambda = 3$. We start by considering the ring integral $R^{(3)}(t) \equiv c_{xi} \mathscr{R}_{ij}^{(3)}(\mathbf{0}, t)\, c_{xj}$, which reads

$$\begin{aligned}
R^{(3)}(t) = {} & \frac{3!}{V^2} A^{(3)}_{i_1 i_2 i_3} A^{(3)}_{j_1 j_2 j_3} \kappa_{j_1} \kappa_{j_2} \kappa_{j_3} \\
& \times \sum_{\mathbf{q}_1 \mathbf{q}_2} \Gamma^0_{i_1 j_1}(\mathbf{q}_1, t)\, S^{-1}_{j_1}(\mathbf{q}_1)\, \Gamma^0_{i_2 j_2}(\mathbf{q}_2, t)\, S^{-1}_{j_2}(\mathbf{q}_2) \\
& \times \Gamma^0_{i_3 j_3}(-\mathbf{q}_1 - \mathbf{q}_2, t)\, S^{-1}_{j_3}(-\mathbf{q}_1 - \mathbf{q}_2) \\
= {} & 6 A^{(3)}_{i_1 i_2 i_3} A^{(3)}_{j_1 j_2 j_3} \kappa_{j_1} \kappa_{j_2} \kappa_{j_3} (\mathbf{1}+\Omega)_{i_1 k_1} (\mathbf{1}+\Omega)_{k_1 k_2} \cdots (\mathbf{1}+\Omega)_{k_{t-1} j_1} \\
& \times (\mathbf{1}+\Omega)_{i_2 l_1} (\mathbf{1}+\Omega)_{l_1 l_2} \cdots (\mathbf{1}+\Omega)_{l_{t-1} j_2} \\
& \times (\mathbf{1}+\Omega)_{i_3 m_1} (\mathbf{1}+\Omega)_{m_1 m_2} \cdots (\mathbf{1}+\Omega)_{m_{t-1} j_3} \\
& \times \delta(\mathbf{r}_{i_1 j_1 \{k\}_t}, \mathbf{r}_{i_3 j_3 \{m\}_t})\, \delta(\mathbf{r}_{i_2 j_2 \{l\}_t}, \mathbf{r}_{i_3 j_3 \{m\}_t}) \\
= {} & 6 A^{(3)}_{i_1 i_2 i_3} Q_{i_1 j_1}(t)\, \kappa_{j_1} Q_{i_2 j_2}(t)\, \kappa_{j_2} Q_{i_3 j_3}(t)\, \kappa_{j_3} A^{(3)}_{j_1 j_2 j_3} \operatorname{odd}(t)
\end{aligned} \tag{4.15}$$

where $Q_{ij}(t)$ is defined in Eq. (4.6). We used the definition $A^{(3)}_{jkl} \equiv c_{xi} \Omega^{(3)}_{ijkl}$. The factorization of the δ's is a consequence of the explicit structure (see Appendix A) of $A^{(3)}$ and Ω, analogous to the calculation of $R^{(2)}(t)$. From expression (4.8) for $Q_{ij}(t)$ in terms of the functions K and L, the contraction in Eq. (4.15) yields [with $T = \frac{1}{2}(t+1)$]

$$\begin{aligned}
R^{(3)}(t) = {} & -32 \kappa_x \kappa_y^2 \operatorname{odd}(t) \\
& \times \{[K(2\kappa_y, T) - L(2\kappa_y, T)][K^2(2\kappa_x, T) + L^2(2\kappa_x, T)]\}
\end{aligned} \tag{4.16}$$

Since we know the explicit form of $K(\lambda, t)$ and $L(\lambda, t)$, the value of $R^{(3)}(t)$ can be evaluated exactly. The same holds for $\phi_x^{(3)}(t)$ in Eq. (3.12).

We have computed exact expressions for ring corrections to the mean field result for the momentum autocorrelation function. The expressions have been evaluated numerically and the results for $D_x^{(2)}$ and $D_x^{(3)}$ in Eq. (3.15) are shown in Fig. 3.

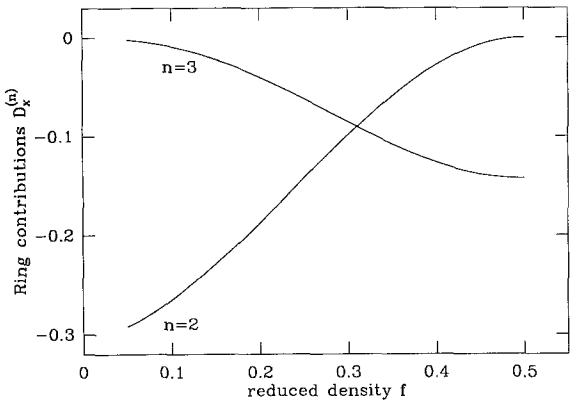

Fig. 3. Ring corrections $D_x^{(n)}$ ($n=2, 3$) of Eq. (3.14) to the collective diffusion coefficient D_x, where $n=2, 3$ denotes the number of correlated particles involved in the one-loop diagrams of Eq. (3.7).

5. ASYMPTOTIC BEHAVIOR

In this section we compute the long-time behavior of $\phi_x^{(\lambda)}(t)$ using a saddle point method. First we treat the case $\lambda=2$, next $\lambda=3$.

As can be seen from Eqs. (3.12), (4.12), and (4.13), the long-time behavior of $\phi_x^{(2)}(t)$ is determined by the long-time behavior of $K(\lambda, t)$ and $L(\lambda, t)$. We will therefore consider an asymptotic expansion of these two functions. The starting point of our analysis is the observation that the combinatorial factor $f(k, n)$ in Eq. (4.11) reaches its maximum in the vicinity of $k \approx n/2$, and is relatively small at $k \approx 0$ and $k \approx n$. As a consequence we expect that the dominant contributions in the expression (4.9) for $K(\lambda, t)$ and $L(\lambda, t)$ do not come from the sum boundaries $s=0, 1,...,$ and $s=t, t-1,...,$ but from $s \approx xt$ $(0<x<1)$. We proceed by converting the discrete sum over s into a (continuous) integration over x, while considering $f(xt, t)$. Stirling's approximation (plus corrections) of the Γ functions gives

$$f(xt, t)=\frac{1}{(2\pi t)^{1/2}}\left(\frac{x}{1-x}\right)^{1/2}[x^{-xt}(1-x)^{-(1-x)t}]$$
$$\times\left[1+\frac{1}{12t}\left(1-\frac{1}{x(1-x)}\right)+O\left(\frac{1}{t^2}\right)\right] \quad (t\to\infty) \qquad (5.1)$$

Substituting Eq. (5.1) and the relation

$$f(xt+1, t)\, f(xt, t)=\frac{1-x}{x} f^2(xt, t)$$

into the definition of $K(\lambda, t)$ and $L(\lambda, t)$ yields

$$K(\lambda,t)=\frac{1}{2\pi\lambda}\int_0^1 dx\frac{x}{1-x}[g(x)]^{2t}\left[1+\frac{1}{6t}\left(1-\frac{1}{x(1-x)}\right)+O\left(\frac{1}{t^2}\right)\right]$$

$$L(\lambda,t)=\frac{1}{2\pi(1-\lambda)}\int_0^1 dx[g(x)]^{2t}\left[1+\frac{1}{6t}\left(1-\frac{1}{x(1-x)}\right)+O\left(\frac{1}{t^2}\right)\right] \tag{5.2}$$

where

$$g(x)=\left(\frac{\lambda}{x}\right)^x\left(\frac{1-\lambda}{1-x}\right)^{1-x} \qquad \left(0<x<1 \text{ and } 0\leqslant\lambda\leqslant\frac{1}{2}\right) \tag{5.3}$$

The function $g(x)$ reaches its maximum value 1 at $x=\lambda$, so that $[g(x)]^{2t}$ $(t\to\infty)$ is a very steep function in the neighborhood of λ, while it is rapidly vanishing away from λ. Therefore we expand $\log[g(x)]$ in stead of $g(x)$ around $x=\lambda$. In Appendix B we show that this saddle point method yields

$$\begin{aligned}K(\lambda,t)&=\frac{1}{2(\pi t)^{1/2}}\left(\frac{\lambda}{1-\lambda}\right)^{1/2}\left[1-\frac{1-13\lambda+13\lambda^2}{24\lambda(1-\lambda)\,t}+O\left(\frac{1}{t^2}\right)\right]\\ L(\lambda,t)&=\frac{1}{2(\pi t)^{1/2}}\left(\frac{\lambda}{1-\lambda}\right)^{1/2}\left[1-\frac{7-13\lambda+13\lambda^2}{24\lambda(1-\lambda)\,t}+O\left(\frac{1}{t^2}\right)\right]\end{aligned} \tag{5.4}$$

Hence Eqs. (4.12) and (4.13) yield the asymptotic behavior of the ring integral:

$$R^{(2)}(t)=-(1-2f_y)^2\frac{\mathrm{odd}(t)}{2\pi t^2}\frac{\kappa_x}{\kappa_y}\frac{1}{D_x^0(D_x^0D_y^0)^{1/2}} \qquad (t\to\infty) \tag{5.5}$$

Here we used $\lambda_\alpha=2\kappa_\alpha$, $D_\alpha^0=1/\omega_\alpha-1/2$, and $\omega_\alpha=4\kappa_{\bar\alpha}$ with $\alpha=x, y$ and $\bar\alpha=y, x$.

From expression (5.5) of the long-time behavior of the ring integral $R^{(2)}(t)$, we can calculate the tail amplitudes of the long-time tail of $\phi_x^{(2)}(t)$. We have already concluded that the ring integral is vanishing for even time arguments, so that in expression (3.12) for $\phi_x^{(2)}(t)$, either the odd or the even τ's contribute, depending on the parity of t. In the limit $t\to\infty$ the ring integral factors out of the τ summation, and hence

$$\phi_x^{(2)}(t)=-\frac{a_\pm}{t^2} \qquad (t\to\infty) \tag{5.6}$$

with tail amplitudes a_+ (t even) and a_- (t odd) given by

$$a_\pm = \frac{(1-2f_y)^2}{4\pi\kappa_y} \frac{\xi_\pm(\omega_x)}{D_x^0(D_x^0 D_y^0)^{1/2}} \tag{5.7}$$

Here

$$\xi_t(\omega) = \begin{cases} \xi_-(\omega) = \dfrac{\omega^2 - 2\omega + 2}{\omega^2(2-\omega)^2} & t \text{ odd} \\ \xi_+(\omega) = \dfrac{2(1-\omega)}{\omega^2(2-\omega)^2} & t \text{ even} \end{cases} \tag{5.8}$$

Note that $a_\pm$ is positive for all ω_x. The two amplitudes represent in fact high-frequency oscillations in $\phi_x^{(2)}(t)$, which are typical for a lattice gas on a square lattice (see, e.g., ref. 8). These oscillations are related to the so-called dynamic staggered invariants, to which we return in a separate publication.[7]

The long-time behavior of $\phi_x^{(3)}(t)$ is determined by the long-time behavior of $R^{(3)}(t)$. Inserting the asymptotic expressions of K and L of Eq. (5.4) into Eq. (4.16) yields $R^{(3)}(t) \sim t^{-5/2}$ $(t \to \infty)$. Therefore $\phi_x^{(3)}(t)$ shows a tail with exponent $-5/2$:

$$\phi_x^{(3)}(t) = -\frac{1}{4\pi^{3/2}} \frac{\xi_t(\omega_x)}{D_x^0 D_y^0 (D_x^0)^{1/2}} \frac{1}{t^{5/2}} \qquad (t \to \infty) \tag{5.9}$$

as follows from Eq. (3.12). Again the amplitudes for even and odd times differ. Note that the long-time limit of $\phi_x(t)$ is determined by $\phi_x^{(2)}(t)$, which has a t^{-2} long-time tail. This tail can be summed [using (3.15)] to give a finite correction to the Boltzmann value (3.6) of the collective diffusion coefficient.

6. COMPUTER SIMULATIONS

The Green–Kubo formalism provides us with a tool to determine the collective diffusion coefficient by means of computer simulations, since it expresses D_x in terms of the time integral (sum) of $\langle P_x(t) P_x(0) \rangle$ [see Eqs. (2.6) and (2.7)]. We recall that $P_x(t)$ denotes the total momentum in the x direction at time t and $\langle \cdots \rangle$ an average over a homogeneous *equilibrium* ensemble. Of course D_x may also be determined by studying the relaxation toward equilibrium of an initial nonequilibrium state.[2] Our procedure, however, avoids the ill-defined aging period following the preparation of a nonequilibrium initial state. Furthermore, it avoids all nonlinear effects, since dissipation coefficients are measured from microscopic fluctuations around a well-defined equilibrium state. We can there-

fore start with a homogeneous equilibrium configuration (where the probability to have a particle in an x channel equals f_x and in a y channel equals f_y for all sites) and calculate the total x momentum $P_x(0)$. Then we let the system evolve in time, while we keep track of $P_x(t)$ for every time t. The quantities of interest are the products $P_x(t)\,P_x(0)$. The average over many initial configurations is a good estimate for $\langle P_x(t)\,P_x(0)\rangle$. The time sum then gives according to Eq. (2.6) an experimental value for D_x, which can be compared with the renormalized transport coefficient, calculated from the ring diagrams. Furthermore, the simulations provide detailed values for the momentum autocorrelation at times $t=0, 1, 2,..., t_{\max}$, which also have been calculated exactly within the approximation of the ring kinetic theory.

It turned out that the available computer power was not enough to obtain sufficiently accurate statistics in the measurement of the momentum autocorrelation function at times larger than about $t_{\max} \simeq 30$. At present it is therefore impossible to observe the theoretically predicted long-time tail of the correlation function. However, the statistics is certainly sufficient to give a good estimate for D_x, since only the first few terms in the Green–Kubo sum contribute substantially (if the density is not extremely low).

The simulations of ref. 2 already indicated that the Boltzmann approximation of D_x overestimates the actual value. This is confirmed by our own simulations, as can be seen in Fig. 2, where we have plotted both D_x^0 (solid line) and the simulated values of D_x (squares) as a function of the reduced density $f \equiv f_x = f_y$. We note that the Boltzmann result deviates about 10% at $f=0.10$ and even 40% at $f=0.50$, consistent with the intuitive argument that recollisions are more significant at higher densities. The measured values are obtained in computer simulations on a 200×200 system. We averaged over 2000 independent initial configurations at each density f. The simulated collective diffusion coefficient are obtained by restricting the Green–Kubo sum to $t \leqslant t_{\max} = 30$, except at $f=0.10$, where $t_{\max}=40$. For longer times the statistics in the measurements of the momentum autocorrelation is too poor, and the numerical contributions are expected to be insignificant.

Once we have obtained the values of D_x for different densities by simulation, we can directly calculate the deviations from the Boltzmann value D_x^0, and compare them with the numerical values of the analytic corrections $D_x^{(\lambda)}$, given by the time sum of $\phi_x^{(\lambda)}(t)$ for $\lambda=2, 3$ in Eqs. (3.15), (4.12), and (4.16). We note that at low densities the correction is determined by $D_x^{(2)}$ only, while at the half-filled lattice the correction to the Boltzmann result is completely given by $D_x^{(3)}$ (see Fig. 3). We have restricted the theoretical Green–Kubo sums to $t \leqslant t_{\max} = 200$, where the

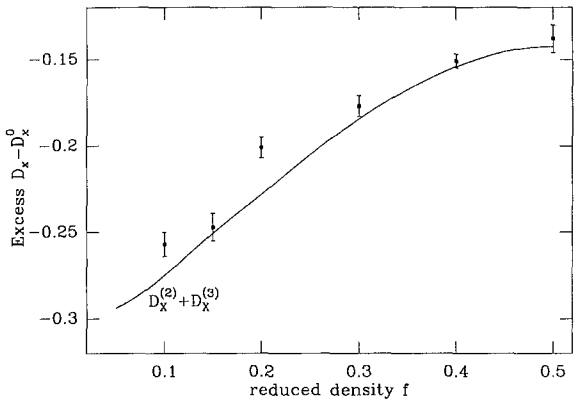

Fig. 4. Excess diffusion coefficient $D_x - D_x^0$ versus reduced density $f = f_x = f_y$, where D_x^0 is the mean field value. The solid line denotes predictions from ring kinetic theory; the squares denote computer simulations on a 200×200 lattice, averaged over 2000 runs per data point.

sums are checked to have converged sufficiently. In Fig. 4 we plot the simulated deviation from the Boltzmann result (squares) and the sum $D_x - D_x^0 = D_x^{(2)} + D_x^{(3)}$ (solid line) as a function of f.

There is a good agreement between theory and simulations at higher densities. At lower densities the simulation data taken at *different* densities do not seem to be consistent with each other, given the error bars (denoting one standard deviation) obtained from 2000 independent runs per density point. It looks as if we largely underestimate the errors, for which we have no explanation at present.

The difference between theory and simulations does not come from the extra summation range for $t \geqslant t_{\max} = 30$ neglected in the simulations. At densities $f = 0.10$ and $f = 0.20$ the neglected terms for $t \geqslant t_{\max}$ contribute only 4% and 1%, respectively, to the total sum in the analytic expression.

For low densities we expect that the simple ring collisions give the dominant corrections to the mean field result. For higher densities, however, in general more complicated collision sequences are of importance. In view of that, the good agreement between theory and experiment at high densities is in fact surprising.

In summary we conclude that the results of the ring kinetic theory applied to this specific diffusive cellular automaton agree on the whole quite well with the simulation data.

7. CONCLUSIONS

The results of this article can be summarized as follows:

1. We have derived explicit expressions for non-mean-field contributions to the momentum autocorrelation function (MACF) $\phi_x(t)$ of a

diffusive two-dimensional lattice gas automaton. They give substantial corrections to the Boltzmann or mean field values for the transport coefficient.

2. The MACF has a leading t^{-2} long-time tail and a subleading $t^{-5/2}$ tail. We have explicit expressions for the tail amplitudes in terms of the reduced densities f_x and f_y. Both tails have a different amplitude for even and odd times. The different tail amplitudes for even and odd times is typical for lattice gases on bipartite lattices, such as the square lattice. Similar phenomena have already been observed in computer simulations of the velocity autocorrelation function in lattice Lorentz gases, where the tail amplitudes at even and odd times differ by an order of magnitude in certain density intervals.[9] The mean field theory predicts an exponential decay, so that the molecular-chaos assumption is no longer valid.

3. The Green-Kubo formula for the collective diffusion coefficient D_x has been calculated from ring kinetic theory. Because the MACF has a t^{-2} long-time tail, the rings give a finite contribution to the collective diffusion coefficient.

4. Computer simulations provide experimental values for the MACF(t) and hence for the collective diffusion coefficient. The Boltzmann value is found to overestimate the actual values by 10–40%, depending on the density considered. Our theoretical corrections to the Boltzmann result are in good agreement with the simulation results.

5. Unfortunately, the theoretically predicted long-time tail in the momentum autocorrelation function could not be detected in the computer simulations. The reason is the poor statistics in the measurements for long times. We have, however, measured a t^{-2} long-time tail in a similar automaton with tagged particle collision rules. This will be reported in a separate publication.[7]

APPENDIX A. COLLECTIVE EXPANSION COEFFICIENTS

In this appendix we give the coefficients $\Omega^{(\lambda)}_{i i_1 \cdots i_\lambda}$ in the expansion, Eq. (2.5), of the collision operator $I_i(n)$ in Eq. (2.2). For $\lambda = 1$ we find

$$\Omega = \Omega^{(1)} = \begin{pmatrix} -2\kappa_y & 0 & 2\kappa_y & 0 \\ 0 & -2\kappa_x & 0 & 2\kappa_x \\ 2\kappa_y & 0 & -2\kappa_y & 0 \\ 0 & 2\kappa_x & 0 & -2\kappa_x \end{pmatrix} \tag{A.1}$$

where $\kappa_\alpha = f_\alpha(1 - f_\alpha)$ with $\alpha = x, y$.

The coefficients for $\lambda = 2, 3$ only occur contracted with c_{xi}. The relevant combinations,

$$c_{xi}\Omega^{(\lambda)}_{ii_1\cdots i_\lambda} = \Omega^{(\lambda)}_{0i_1\cdots i_\lambda} - \Omega^{(\lambda)}_{2i_1\cdots i_\lambda} \equiv A^{(\lambda)}_{i_1\cdots i_\lambda} \tag{A.2}$$

are symmetric in the labels $(i_1 \cdots i_\lambda)$. This yields for $\lambda = 2$

$$A^{(2)} = (1-2f_y)\begin{pmatrix} 0 & -1 & 0 & -1 \\ -1 & 0 & 1 & 0 \\ 0 & 1 & 0 & 1 \\ -1 & 0 & 1 & 0 \end{pmatrix} \tag{A.3}$$

In $A^{(3)}_{jkl}$ the only nonvanishing elements are

$$A^{(3)}_{\pi(0,1,3)} = -A^{(3)}_{\pi(2,1,3)} = \tfrac{2}{3} \tag{A.4}$$

where $\pi(i, j, k)$ is a permutation of the integers i, j, k.

APPENDIX B. LONG-TIME BEHAVIOR OF *K* AND *L*

In this appendix we derive the long-time behavior of the functions $K(\lambda, t)$ and $L(\lambda, t)$, quoted in Eq. (5.4). K and L will turn out to be identical to the dominant $(1/\sqrt{t})$ order as $t \to \infty$, so that it is necessary to calculate the next order in $[K(\lambda_1, t) + L(\lambda_1, t)][K(\lambda_2, t) - L(\lambda_2, t)]$ [see Eq. (4.13)]. The observation that the function $[g(x)]^{2t}$ present in expression (5.2) is very steep near its maximum at $x = \lambda$ for $t \to \infty$ indicates a poor convergence of the Taylor series around this point. It seems, therefore, more attractive to expand $\log[g(x)]$, which yields

$$\log[g(x)] = h(x-\lambda) + O[(x-\lambda)^5] \tag{B.1}$$

where

$$h(y) = -\frac{1}{2\lambda(1-\lambda)}\, y^2 + \frac{1-2\lambda}{6\lambda^2(1-\lambda)^2}\, y^3 - \frac{1-3\lambda+3\lambda^2}{12\lambda^3(1-\lambda)^3}\, y^4 \tag{B.2}$$

For the moment we will concentrate on $K(\lambda, t)$.

Defining $p(y) = \exp\{-y^2/[2\lambda(1-\lambda)]\}$, which in fact equals $g(x)$ in lowest order (where $y = x - \lambda$), and using the identity $a = (a-b) + b$ we see from Eq. (5.2) that

$$K(\lambda, t) = K_1(\lambda, t) + K_2(\lambda, t) \tag{B.3}$$

where

$$K_1(\lambda, t) = \frac{1}{2\pi\lambda} \int_{-\lambda}^{1-\lambda} dy \frac{\lambda + y}{1 - \lambda - y} [g(y)^{2t} - p(y)^{2t}] \times [1 + O(t^{-1})] \tag{B.4}$$

$$K_2(\lambda, t) = \frac{1}{2\pi\lambda} \int_{-\lambda}^{1-\lambda} dy \frac{\lambda + y}{1 - \lambda - y} p(y)^{2t} \times \left[1 + \frac{1}{6t}\left(1 - \frac{1}{(y+\lambda)(1-y-\lambda)}\right) + O(t^{-2})\right] \tag{B.5}$$

with $y = x - \lambda$. The reason that we do not take into account the $O(t^{-1})$ term in Eq. (B.4), whereas we do in Eq. (B.5), is the fact that $K_2(\lambda, t)$ contains the dominant (zeroth-order) contribution, so that the $O(t^{-1})$ term contributes to the first-order corrections. The $O(t^{-1})$ term present in the expression for $K_1(\lambda, t)$ would give rise to a correction of second order, and may therefore be omitted.

Using the Taylor expansions

$$\frac{\lambda + y}{1 - \lambda - y} = \frac{\lambda}{1-\lambda} + \frac{y}{(1-\lambda)^2} + \frac{y^2}{(1-\lambda)^3} + O(y^3) \tag{B.6}$$

and

$$g(y)^{2t} - p(y)^{2t} = \exp\left[-\frac{y^2 t}{\lambda(1-\lambda)}\right] \times \left[\frac{(1-2\lambda)\, t}{3\lambda^2(1-\lambda)^2} y^3 - \frac{(1 - 3\lambda + 3\lambda^2)\, t}{6\lambda^3(1-\lambda)^3} y^4 + O(y^5)\right] \tag{B.7}$$

together with $\int_{-\infty}^{\infty} dz\, z^4 \exp(-z^2) = \frac{3}{4}\sqrt{\pi}$, yields

$$K_1(\lambda, t) = \frac{1}{2(\pi t)^{1/2}} \left(\frac{\lambda}{1-\lambda}\right)^{1/2} \left[\frac{1 - \lambda - 3\lambda^2}{8\lambda(1-\lambda)\, t}\right] + O(t^{-5/2}) \tag{B.8}$$

$$K_2(\lambda, t) = \frac{1}{2(\pi t)^{1/2}} \left(\frac{\lambda}{1-\lambda}\right)^{1/2} \left[1 - \frac{1 - 4\lambda + \lambda^2}{6\lambda(1-\lambda)\, t}\right] + O(t^{-5/2}) \tag{B.9}$$

Adding the two results [see Eq. (B.3)] indeed gives the already mentioned asymptotic behavior of $K(\lambda, t)$.

A similar splitting can be done for $L(\lambda, t)$:

$$L(\lambda, t) = L_1(\lambda, t) + L_2(\lambda, t) \tag{B.10}$$

where

$$L_1(\lambda, t) = \frac{1}{2\pi(1-\lambda)} \int_{-\lambda}^{1-\lambda} dy [g(y)^{2t} - p(y)^{2t}][1 + O(t^{-1})] \quad \text{(B.11)}$$

$$L_2(\lambda, t) = \frac{1}{2\pi(1-\lambda)} \int_{-\lambda}^{1-\lambda} dy\, p(y)^{2t} \times \left[1 + \frac{1}{6t}\left(1 - \frac{1}{(y+\lambda)(1-y-\lambda)}\right) + O(t^{-2})\right] \quad \text{(B.12)}$$

The same line of argument can be followed as in the calculation of $K(\lambda, t)$:

$$L_1(\lambda, t) = -\frac{1}{2(\pi t)^{1/2}} \left(\frac{\lambda}{1-\lambda}\right)^{1/2} \left[\frac{1 - 3\lambda + 3\lambda^2}{8\lambda(1-\lambda)\, t}\right] + O(t^{-5/2}) \quad \text{(B.13)}$$

$$L_2(\lambda, t) = \frac{1}{2(\pi t)^{1/2}} \left(\frac{\lambda}{1-\lambda}\right)^{1/2} \left[1 - \frac{1 - \lambda + \lambda^2}{6\lambda(1-\lambda)\, t}\right] + O(t^{-5/2}) \quad \text{(B.14)}$$

From Eq. (B.10) we easily verify that Eq. (5.4) indeed represents the long-time behavior of $L(\lambda, t)$ up to the desired order.

ACKNOWLEDGMENTS

We are indebted to B. M. Boghosian, J. W. Dufty, and D. Frenkel for helpful discussions and M. A. van der Hoef for providing computer programs and for careful reading of the manuscript.

REFERENCES

1. M. M. Kops-Werkhoven, A. Vrij, and H. N. W. Lekkerkerker, *J. Chem. Phys.* **78**:2760 (1983).
2. B. M. Boghosian and C. D. Levermore, in *Discrete Kinetic Theory, Lattice Gas Dynamics and Foundations of Hydrodynamics*, R. Monaco, ed. (World Scientific, Singapore, 1989), p. 44.
3. W. Taylor and B. M. Boghosian, unpublished.
4. T. R. Kirkpatrick and M. H. Ernst, *Phys. Rev. A* **44**:8051 (1991).
5. M. H. Ernst and J. W. Dufty, *J. Stat. Phys.* **58**:57 (1990).
6. M. H. Ernst, in *Liquids, Freezing and the Glass Transition*, D. Levesque, J. P. Hansen, and J. Zinn-Justin, eds. (Elsevier Science, Amsterdam, 1991), p. 43.
7. R. van Roij and M. H. Ernst, preprint (August 1992).
8. M. H. Ernst, in *Ordering Phenomena in Condensed Matter Physics*, Z. M. Galasiewicz and A. Pękalski, eds. (World Scientific, Singapore, 1991), p. 291.
9. P. M. Binder and D. Frenkel, *Phys. Rev. A* **42**:2463 (1990).